Colloids and Surfaces B: Biointerfaces 208 (2021) 112091

Contents lists available at ScienceDirect

Colloids and Surfaces B: Biointerfaces

journal homepage: www.elsevier.com/locate/colsurfb

Switch off inflammation in spleen cells with CD40-targeted PLGA nanoparticles containing dimethyl fumarate

Sahar khosravi [a], Hassan Bardania [b,c], Reza Mansouri [a,*], Mohammad Taher Tahoori [a,*], Fereshte Ghafari [a], Adel Mohammadzdeh [d], Mohamad Hassan Fouani [e], Ali Akbar Pourfathollah [f], Masoud Soleimani [g]

[a] Department of Immunology, Faculty of Medicine, Shahid Sadoughi University of Medical Sciences and Health Services, Yazd, Iran
[b] Cellular and Molecular Research Center, Yasuj University of Medical Sciences, Yasuj, Iran
[c] Clinical Research Development Unit, Imamsajad Hospital, Yasuj University of Medical Sciences, Yasuj, Iran
[d] Department of Immunology and Genetic, Urmia University of Medical Sciences, Urmia, Iran
[e] Department of Nanobiotechnology, Faculty of Biological Sciences, Tarbiat Modares University, Tehran, Iran
[f] Department of Immunology, Faculty of Medical Sciences, Tarbiat Modares University, Tehran, Iran
[g] Department of Hematology, Faculty of Medical Sciences, Tarbiat Modares University, Tehran, Iran

ARTICLE INFO

Keywords:
Spleen cells
PLGA
DMF
Multiple sclerosis
mAbCD40

ABSTRACT

The purpose of this study was designing and synthesizing a PLGA formulation targeted with anti-CD40 monoclonal antibody, which has suitable physicochemical properties as a dimethyl fumarate (DMF) drug delivery system having minimal cytotoxicity. Therefore, this research was performed to determine the effect of anti-CD40mAb-DMF-NPs on the expression of IL-1β, IL-6 and TNF-α cytokine genes in mouse splenocytes. The toxicity of different groups, namely free PLGA, free DMF, DMF-containing PLGA, anti-CD40mAb-DMF-NPs, was evaluated by MTT assay. PLGA formulations conjugated with mAbCD40 were loaded with DMF drug that showed little cytotoxic effect against mouse splenocytes. QRT-PCR method was subsequently used to assess the effect of the mentioned groups on the expression of IL-1β, TNF-α and IL-6 genes. After treatment of the cells with DMF alone or with polymer carriers, the expression of IL-1β, IL-6 and TNF-α cytokine genes was significantly reduced. The decrease in expression was markedly higher in the antibody-targeted nanoparticles group relative to other treatment groups. Our results in this area are promising and provide a good basis for further future studies in this regard.

1. Introduction

Multiple sclerosis (MS) is a progressive inflammatory autoimmune disease and a major cause of disability among young adults, with an average age of onset at 30 years [1]. Current MS treatment methods mainly focus on reducing the inflammatory activity of the disease [2]. However, decreased disease activity, especially delaying disease progression, is not always satisfactory and more effective compounds could lead to serious side effects. Therefore, there is great need in medical field for new effective and safe treatment methods [3].

Fumaric acid esters (FAEs) such as dimethyl fumarate (DMF) have received extensive interest in MS treatment [4]. FAE was initially prescribed for psoriasis treatment, while DMF, originally marketed as Tecfidera in the form of hard gelatin capsules, has recently proved useful for the treatment of progressive MS as well as relapsing-remitting multiple sclerosis (RRMS) [4–6].

Tecfidera exhibits various side effects including flushing, gastrointestinal discomfort, as well as more serious side effects, such as renal toxicity and lymphopenia [6,7]. However, two capsules of Tecfidera should be administered per day to achieve sustained efficacy [8,9].

Drug delivery systems are evolving at a fast space, and novel technologies are introduced in order to reduce systemic side effects through delivering the therapeutic agent to the desired targeted site. Moreover, novel drug formulations exhibit several advantages over conventional formulations, such as controlled release of active compounds, reduction of drug dose and frequency of administrations [10–14]. Drug delivery nanosystems offer solutions for the targeted transportation of bioactive molecules, solubility modification, bioavailability improvement and

* Corresponding authors.
E-mail addresses: hasan.bardania@yums.ac.ir (H. Bardania), rmm542003@yahoo.com (R. Mansouri), immuno.2006@yahoo.com (M.T. Tahoori).

https://doi.org/10.1016/j.colsurfb.2021.112091
Received 6 April 2021; Received in revised form 26 August 2021; Accepted 31 August 2021
Available online 1 September 2021

trespassing barriers such as such as the blood brain barrier (BBB) and the blood–cerebrospinal fluid barrier (BCSFB) [15]. For the synthesis of drug delivery nanosystems, researchers have employed various natural and synthetic polymers such as poly(ε-caprolactone) (PLE), poly(vinyl alcohol) (PVA), poly(*N*-vinylpyrrolidone) (PVP), poly(lactic acid) (PLA), poly(lactic-co-glycolic acid) (PLGA), chitosan, gelatin, hyaluronate, alginate, collagen, and silica [16]. Targeted drug delivery could be achieved through surface modification of drug delivery vehicles using targeting ligands such as small molecules, oligosaccharides, peptides, proteins, antibodies, and aptamers.

Monoclonal antibodies are among the targeting ligands used to functionalize nanoparticles [14]. Anti-CD40 monoclonal antibody used in this study is often used to target CD40 expressing blood cells involved in innate immunity such as B cells, macrophages, and dendritic cells [17].

The spleen is a combination of innate and acquired immune systems that are organized in a unique way. In addition to playing a role in the immune response, spleen is an important lymphatic organ in the regulation of the immune system, in which many immune cells are located and are sensitive to antigens [18,19]. It is also responsible for the maturation of blood cells and immunity. Leukocytes in the spleen involve different B- and T-cell types, as well as DCs and macrophages that show different functions. However, the spleen is an intelligent organ regulating the immune system in close contact with the brain [20–22].

The goal of this study was to design and synthesize a PLGA formulation targeted with CD40 monoclonal antibody having acceptable physicochemical properties as a DMF drug delivery system associated with minimal cytotoxicity, which is a promising solution to increase drug delivery efficiency. In the present research, nanoparticles were synthesized through oil in water (o/w) single emulsion solvent evaporation method [23,24], and their morphological properties were examined by SEM. Splenocytes from C57BL/6 mice were exposed to LPS as well as to the drug encapsulated within nanoparticles in vitro and the expression of IL-6, IL-1β and TNF-α cytokines in cells was evaluated [25]. Because the spleen is the main filter of pathogens and antigens in the blood, our goal is to investigate the involvement of spleen in the regulation of immune responses as well as its association with inflammatory diseases such as MS. The results show that trapping the drug within nanoparticles is more effective than free drug forms. In a similar study, S. Ojha et al. synthesized and statistically optimized DMF loaded in solid lipid nanoparticles (SLN) for better management of multiple sclerosis (MS), the results of which indicated that controlled release DMFs could be a promising candidate for management of multiple sclerosis. In vivo studies should be performed in the future to evaluate the effectiveness of the formulation for control of disease [26]. In 2019, Smriti Ojha et al. performed a study on chitosan polymer nanoparticles loaded with dimethyl fumarate to protect nerves in MS. Finally, PLGA is one of the most widely used polymers for this purpose [27] due to its biodegradability and biocompatibility of degraded materials as well as FDA approval, which is also used in the present study.

2. Materials and methods

2.1. Chemicals

PLGA copolymer (50:50 Purasorb® PDLG 5002A), Poly(vinyl alcohol) (PVA) (87 %–90 % hydrolyzed, MW ~ 30–70 kDa), Morpholinoethanesulfonic acid (MES), 1-ethyl-3-(3-dimethylaminopropyl) carbodiimide hydrochloride (EDC) and 8-*N*-hydroxysulfosuccinimide (NHS) were purchased from Sigma-Aldrich Co. (Sigma-Aldrich, Germany). Anti-CD40 monoclonal antibody (CD40-MA), clone1C10, Catalog Number: MAB5607, was purchased from Abnova. Ethyl acetate was purchased from Merck (Merck, Germany). Thiazolyl blue tetrazolium bromide 98 % (MTT), 3-(4,5-dimethyl-2-thiazolyl)-2,5- diphenyl-2*H*-tetrazolium bromide (MTT reagent), Dimethyl sulfoxide (DMSO), Dimethyl fumarate (DMF) and Phosphate buffered saline (PBS) tablets were from Sigma, Germany. (RPMI 1640 with L-glutamine), Fetal bovine serum, penicillin-streptomycin (10,000 U/mL) were purchased from Gibco Co. (USA). All solutions were prepared using deionized water (Arium Pro, Sartorius AG, Göttingen, Germany).

2.2. Preparation of nanoparticles

PLGA-containing dimethyl fumarate (DMF) formulations were prepared using oil in water (o/w) single emulsion solvent evaporation method. According to the standard method, 20 mg of PLGA was dissolved in 1 mL of ethyl acetate and then added to 4 mL of a 2 % (w/v) aqueous solution of (PVA). The emulsion formed was then homogenized using a sonicator (Ultrasonic Farazot Iran, Sonics & Material Inc., Newtown, CT, USA) in 50 % range for 180 s. Subsequently, 5 mL of 0.2 % (w/v) aqueous solution of (PVA) was added to the previous emulsion and the organic solvent was removed using a rotary evaporation for 45 min (400 mPa, 250 rpm, 30 °C). The nanoparticles were subsequently recovered by centrifugation (13,000 *g*, 30 min, 4 °C) and washed three times with distilled water. After final resuspension, the nanoparticles were transferred to aluminum-covered vials and stored at 4 °C until further analysis. The same method was used to encapsulate dimethyl fumarate within PLGA-NP by adding 2 mg of DMF to the previous components. An outline of the preparation process is shown in the Fig. 1.

2.3. Conjugation of anti-CD40-MA to PLGA-NP

Anti-CD40-MAs were conjugated to PLGA-NPs surface through an amide bond using EDC and NHS. To this aime, 1 mL of pure nanoparticles were centrifuged (13,000 rpm, 30 min, 4 °C) and resuspended in 1 mL of MES buffer (pH = 5.0). The pH was kept at 5 to maximize EDC binding to carboxyl groups of PLGA. Activation was done by adding 200 μL of 0.1 M EDC and 200 μL of 0.7 M NHS (both solved in MES buffer, pH = 5.0) to 200 μL of nanoparticle suspension; the mixture was stirred at room temperature under moderate pressure for 2 h. In order to remove residual reagents, the nanoparticles were centrifuged together with activated carboxyl groups (13,000 rpm, 30 min, 4 °C) and resuspended in PBS. For the formation of amide bond between anti-CD40-MAs and carboxyl groups on PLGA-NPs' surface, 10 μL [0.5 μg/μl] of anti-CD40-MA were added to PLGA-NPs with activated carboxyl groups. After homogenization by microfusion, the mixture was incubated for 4 h at 4 °C. Subsequently, the mixture was centrifuged (13,000 rpm, 30 min, 4 °C) to eliminate excess unbound antibodies and residual reagents.

2.4. Physicochemical characterization of the complex

The size, zeta potential and polydispersity index of PLGA- DMF formulations were assessed by dynamic light scattering (DLS) instrument (Zeta & Size VASCO) at room temperature. Samples were initially diluted with double distilled water. All measurements were performed in triplicates.

2.5. Morphology of PLGA nanoparticles

Using a throw-over device (SEM FEI Quanta 200, ETH, Zurich), a dried thin layer of the prepared samples were coated with gold by mean of physical method of vapor deposition to render samples electrically conductive. The combination of argon gas and gold ions with positive charge was physically placed on the negatively charged surface of the sample. Images were then obtained by scanning electron microscopy with a maximum voltage of 25 kV using KYKY (EM3200 model, China).

2.6. Encapsulation efficiency of PLGA nanoparticles

OD of the supernatant from centrifuging the drug-containing nanoparticle was measured at a maximum wavelength of 235 (control =

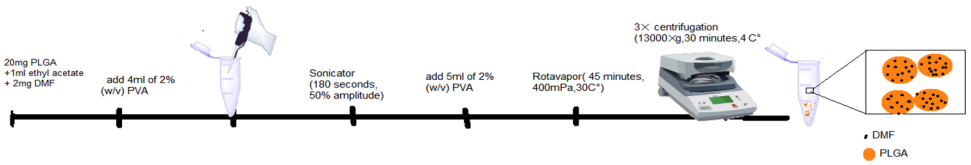

Fig. 1. Schematic representation of nanoparticles preparation using a solvent emulsification-evaporation method based on an oil in water single emulsion technique1 Schema.

distilled water). Using the standard OD curve and the resulting equation, the concentration of the solution and the drug contained in it were calculated. Then, using the obtained information and the following formula, the encapsulation efficiency was *calculated.*

$$\frac{\text{Initial drug concentration-x value}}{\textit{Initial drug concentration}} = \text{Encapsulation efficiency}$$

2.7. DMF release efficiency of PLGA nanoparticle

Phosphate buffer solution (PBS) was used as the release medium to evaluate drug release in vitro. Drug-containing nanoparticles were dissolved in 4 mL of PBS buffer containing 0.5 % SDS (0.5 *g* SDS in 100 mL PBS). After 1, 2, 3, 6, 12, 24, 48, 72 and 96 h' time intervals, samples were centrifuged (13,000 *g*, 30 min, 4 °C), 3 mL of the supernatant was removed and replaced with the same volume of fresh phosphate solution. Then the amount of drug released in buffer medium at each step was measured by spectrophotometry analysis.

2.8. Cell separation

C57 mice were purchased from Yazd Infertility Center and sacrificed by observing ethical points (IR.SSU.MEDICINE.REC.1397.128). The spleen was removed from its site and placed in a Petri dish containing RPMI 1640 medium (10 % FBS, 1 % Pen-Strep). The splenocytes were expelled with a syringe containing the culture medium and isolated using a 70-μm cell strainer. The cells were then transferred to a 15 mL Falcon tube and centrifuged (175 *g* for 5 min at 25 ° C). The supernatant was discarded and the cell pellet homogenized by shaking. Approximately 4 mL of ACK buffer (lysis buffer) was added and kept at room temperature for 3–4 min. Subsequently, to neutralize and remove the lysis buffer, 4–5 mL of culture medium was added and the mixture was centrifuged (175 *g* for 5 min at 25 ° C). The supernatant was discarded and 1–2 mL of culture medium was added to the cell pellet and homogenized. Then, cell count was performed using a hemocytometer and trypan blue dye.

2.9. In-vitro assessment of PLGA-NPs' cytotoxicity

In-vitro cytotoxicity of various PLGA-NP formulation was assessed using MTT colorimetric assay. To this aim, cells seeded in a 96-well plate (2 * 10^5 cells/well) were grown in RPMI 1640 medium supplemented with 10 % fetal bovine serum, penicillin (100 U/mL) and streptomycin (100 g/mL); cell were not grown overnight prior to treatment due to non-adhesive cells. Cell were treated with various concentrations of free PLGA-NPs (100, 10, 1, 0.1, 0.01 μM), free DMF (50, 30, 10, 1 μM) [28], PLGA- DMF-NPs (100, 10, 1, 0.1, 0.01 μM) and PLGA- DMF-anti-CD40-MA-NPs conjugated (100, 10, 1, 0.1, 0.01 μM). Treatment period lasted for 48 and 72 h in 5 % CO_2 at 37 °C in a humidified atmosphere. At the end of treatment period, 20 μL of MTT solution (5 mg/mL) was added to each well, and incubated for 4 h in the dark under the previous conditions. The plate was subsequently centrifuged and the supernatant was discarded. Subsequently, 100 μL of DMSO were added to each well in order to dissolve resulting formazan crystals; absorbance of the obtained solution was recorded at 570 nm using a plate reader Assay was performed in triplicate for each sample.

2.10. Evaluation of IL-1, 1L-6 and TNF-α cytokine genes in comparison with β-actin housekeeping gene

In this study, the expression of IL-1β, 1L-6 and TNF-α genes in mouse splenocytes was investigated by Relative Quantitative-PCR method.

In a 12-well plate, cells (1*10^6 cells/well) were grown in RPMI 1640 medium supplemented with 10 % FBS and penicillin (100 U/mL) and streptomycin (100 g/mL). Culture medium was containing 10 ng/mL LPS (L4391)] to stimulate cells (29, 30). After incubation for 12 h in 5 % CO_2 at 37 °C in a humidified atmosphere, the cells were treated with various PLGA-NP formulations (Un-treated cells, PLGA-NPs, Free DMF, PLGA-DMF-NPs and PLGA-DMF-Ab-NPs groups). At the end of cell treatment period (48 and 72 h), the RNA of the cells was extracted by TRIzol and converted to cDNA using random hexamer primers. Quantitative changes in mRNA level were calculated by RT-PCR under the following conditions: 40 denaturation cycles at 95 °C for 30 s, annealing at 59–61 °C for 30 s depending on the specific set of primers and elongation at 72 °C for 30 s. The reactions were performed at a volume of 10 μL in the presence of SYBR Green on Corbett Rotor-Gen device (Corbett Research, Mortlake, NSW, Australia). The primers used in this study are listed in Table 1.

2.11. Statistical analysis

All experiments were performed in triplicates. Using Graphed Prism 8 software, it was determined that qRT-PCR data obtained from this study had a normal distribution and that parametric tests should be used for them. Comparison was performed using ONE-WAY ANOVA for dose-response curve (analysis of variance using Tukey's test) at significance level of $p < 0.05$. The results were reported as mean ± standard deviation for at least three independent experiments.

3. Results

3.1. Physicochemical properties of nanoparticles

Based on the intensity parameter, the hydrodynamic diameter of different PLGA-NPs was determined obtained using a DLS. Table 2 shows the hydrodynamic diameter and particle dispersion index (PDI) of nanoparticles according to the intensity parameter; the zeta potential of

Table 1
Specifications of Real-time PCR primers.

PCR cycles	bp	Primer sequence (5'->3')	NCBI entry	Gene
40	92	F: AGCCCACCAAGAACGATAGTC R: GCATCAGTCCCAAGAAGGC	NM_031168.2	Il-6 Il-6
40	139	F: GGTGCCTATGTCTCAGCCTCTT R: GCCATAGAACTGATGAGAGGGAG	NM_001278601.1	TNF-α TNF-α
40	148	F: TGGACCTTCCAGGATGAGGACA R:GTTCATCTCGGAGCCTGTAGTG	NM_008361.4	Il-1β IL-1β
40	150	F: AGGGAAATCGTGCGTGACAT R: GAACCGCTCGTTGCCAATAG	NM_007393.5	β-actin β-actin

Table 2
Mean hydrodynamic diameter, zeta potential and dispersion index of nanoparticles.

Particle distribution index (PDI)	Zeta potential (mv)	Mean hydrodynamic diameter (nm)	Particles
0.092	−18	166.6	Free PLGA-NPS
0.02183	−5.76	317	PLGA- DMF-NPs
0.265	−0.1	428	PLGA- DMF-anti-CD40-MA-NPs

the nanoparticles can also be observed. The dispersion indices were between 0.1 and 0.3, indicating that nanoparticles produced exhibit uniform size distribution. Fig. 2 shows PLGA- DMF- anti-CD40-MA-NPs recorded by SEM.

3.2. Drug encapsulation efficiency

Encapsulation efficiency of PLGA-NPs was measured by UV–vis spectroscopy. As shown in Table3, encapsulation efficiency of PLGA-NPs measured equals to 69 %.

3.3. In-vitro DMF release profile

Fig. 3, depicts DMF loaded PLGA-NPs profile release over 100 h. As can be seen in Fig. 3, within the first 60 min of release, mean release rate of DMF from PLGA-NPs is 11 %, and reaches its highest rate ~ 60 % after 100 h. The release pattern shows a slow discharge of the drug from nanoparticles at any point in time.

3.4. In-vitro assessment of PLGA- DMF-NPs safety and biocompatibility

As depicted in Fig. 4A, treatment of mouse splenocytes with various concentrations of free PLGA-NPs, PLGA- DMF-NPs, and PLGA- DMF-anti-CD40-MA-NPs for 48 h caused cell viability to drop X%, Y% and Z% respectively. The extension of the treatment period with various concentrations of free PLGA-NPs, PLGA- DMF-NPs, and PLGA- DMF- anti-CD40-MA-NPs caused further drop in cell viability (X%, Y% and Z% respectively) (Fig. 4B). Moreover, treatment of splenocytes with free DMF for either 48 or 72 h exhibited the highest cell toxicity rates in a concentration dependent manner (Fig. 4A, B).

3.5. RT-PCR

As shown in Fig. 5, free PLGA-NPs did not alter the expression pattern of target genes (TNF-α, IL-1β and IL-6) in a significant manner. However, exposure to DMF formulations induced decrease in the expression rate of the studied genes in a time dependent manner, where

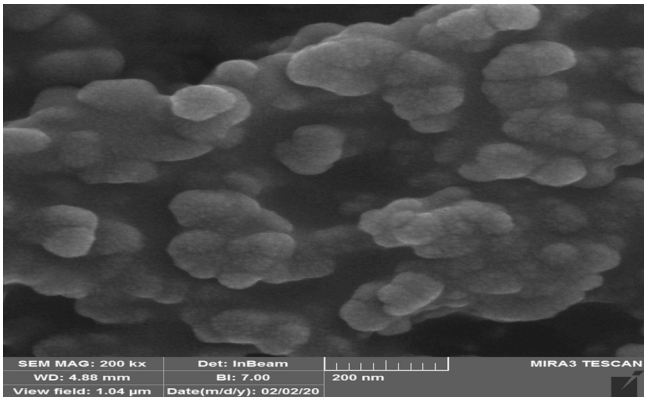

Fig. 2. SEM image of PLGA- DMF- anti-CD40-MA-NPs.

Table 3
Percentage of DMF drug loading efficiency in PLGA nanoparticles.

Loading efficiency (%)	Initial concentration of DMF drug in formulation preparation (µg/mL)	DMF concentration in formulation (µg/mL)
69	2000	1380

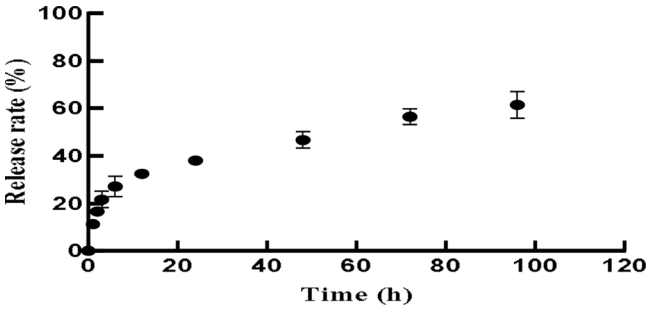

Fig. 3. DMF drug release curve from nanoparticles up to 96 h at 37 °C in PBS buffer.

free DMF caused the least repression and DMF loaded into anti-CD40 functionalized PLGA-NPs exerted the highest repression rates.

4. Discussion

To date, there has been no specific study to trap dimethyl fumarate drug within PLGA nanoparticles. However, several investigations have been performed to trap DMF in other carriers. For instance, Smriti Ojha et al. conducted a research to synthesize and optimize DMF-loaded chitosan nanoparticles by designing box behnken (BBD) to provide a drug delivery system for the management and treatment of MS [28], however, in-vitro or in-vivo assessment of nanoparticles was not reported. Smriti Ojha and colleagues also trapped DMF drug within chitosan (CS) dextran sulphate (DS) nanoparticles.

The PLGA formulation targeted with CD40 monoclonal antibody having suitable physicochemical properties as a DMF drug delivery system exhibited minimal cytotoxicity and significantly decreased the expression of IL-6, IL-1β and TNF-α genes in splenocytes. All components of the designed NPs, namely PLGA, DMF (drug therapy) and anti-CD40 antibody (for targeting APCs), must be effectively integrated into the nanoparticle system without significantly changing the known properties of drug delivery.

The assessment of the physical properties such as morphology, charge and size of a drug delivery system, nanoparticles in this case, is of paramount importance since can influence its stability and biological fate. For instance, peripheral dendritic cells efficiently phagocytose particles ranging from 200 nm to 10 µm. Moreover, although uptake efficiency is enhanced with increased size, but particles with smaller size are more efficiently trapped into lymph nodes [16]. Based on DLS results, the average size of conjugated nanoparticles was nearly 428 nm, but the particle size observed by electron microscopy was approximately 100−200 nm that was comparable to previous studies [14,29,30].

Regarding surface charge, all tested formulations exhibited negative surface charge, which could be attributed to terminal carboxyl group ; the net negative charge helps stabilize hydrophobic particles in water and prevents aggregation [31,32]. Zeta potential values in the formulations decreased upon anti-CD40-mAb conjugation. Antibodies are conjugated to PLGA-NPs surfaces via an amide bond between antibody amine group and PLGA carboxyl group, therefore, resulting in lower negative surface charge in comparison to bare PLGA-NPs [23,24]. Moreover, PLGA-NPs with negative surface charge are more desirable since PLGA-NPs with positive surface charge are cytotoxic [33].

The rate of nanoparticles endocytosis is governed by particles'

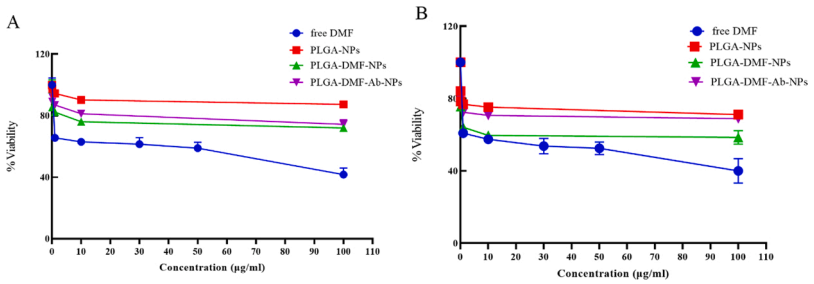

Fig. 4. Survival rate was measured by MTT assay on mouse splenocytes. Optical density value was obtained for free drug, drug loaded within PLGA and Ab-PLGA-DMF at 100 % viability (0 % cytotoxicity).

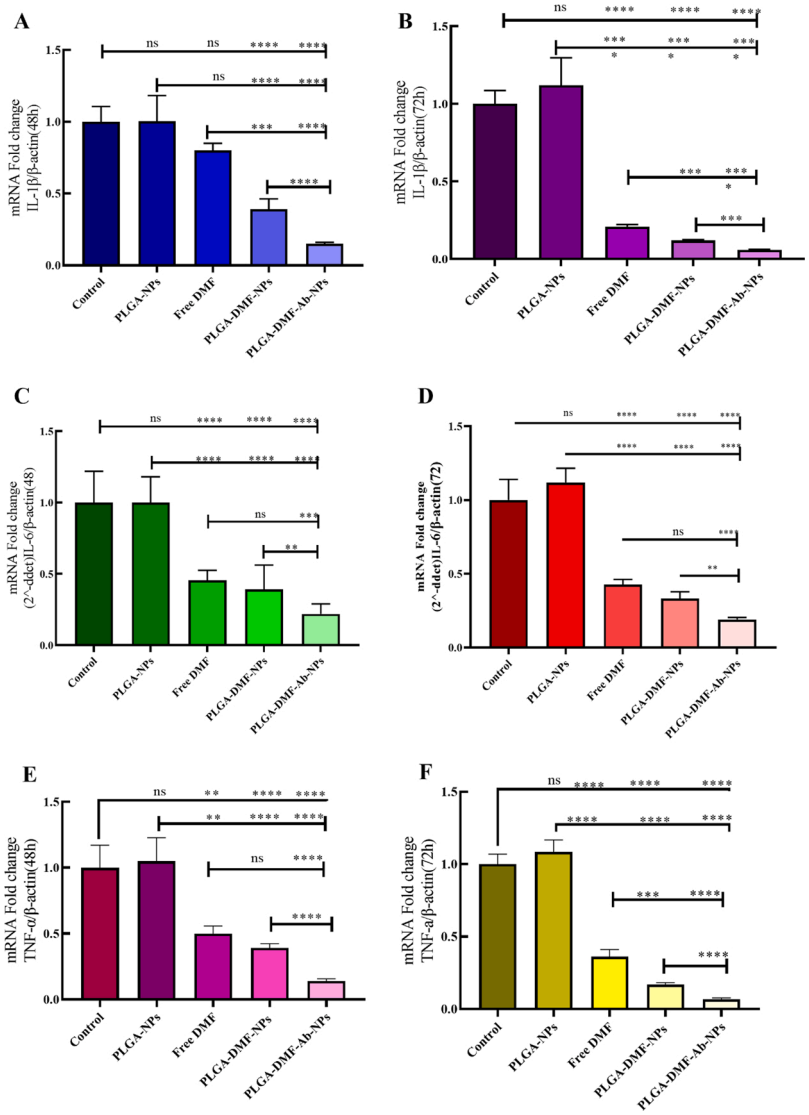

Fig. 5. A-B: Evaluation of IL-1β gene expression in the studied groups during 48 and 72 h. Error bars represent the SEM. Using One way-ANOVA test, there was a significant difference with one star ($p < 0.05$), with two stars ($p < 0.01$), with three stars ($p < 0.001$) and with four stars ($p < 0.0001$) between mean ΔCT of groups.

C–D: Evaluation of IL-6 gene expression in the studied groups during 48 and 72 h. Error bars represent the SEM. Using One way-ANOVA test, there was a significant difference with one star ($p < 0.05$), with two stars ($p < 0.01$), with three stars ($p < 0.001$) and with four stars ($p < 0.0001$) between mean ΔCT of groups.

E–F: Evaluation of TNF-α gene expression in the studied groups during 48 and 72 h. Error bars represent the SEM. Using One way-ANOVA test, there was a significant difference with one star ($p < 0.05$), with two stars ($p < 0.01$), with three stars ($p < 0.001$) and with four stars ($p < 0.0001$) between mean ΔCT of groups.

surface degree of roughness. Schrade et al. demonstrated that nanoparticles with rough surface were internalized by the cells more slowly in comparison to nanoparticles with smooth surface [34]. Scanning electron micrographs (SEMs) enable the collection of information regarding surface morphology of nanoparticles. The image shows the spherical shape of NPs as well as their smooth pore free surface [24].

Drug release data for PLGA nanoparticles containing DMF under optimal conditions were reported as mean ± SD. The release of drug under normal conditions (37 °C and pH = 7.4) is continuous and controlled so that only 38 % of the drug was released within the first 24 h. As can be seen, the slope and release of the drug gradually decreases such that the slope of curve in terms of release is close to zero up to 96 h. In a similar study on Sitagliptin release from PLGA-NPs, initially 15 % of the release took place successively. Subsequently, 67 % of the drug was released within 24 h and 96 % within 48 h. Rapid drug release may be related to nanoparticle surface drug with soluble medium. It was clear that the drug composition in PLGA nanoparticles could be significantly stable [30]. In another study, Smriti Ojha et al. reported the synthesis of

DMF loaded chitosan NPs for the management of MS, drug release was reported to be 84 % in the first 24 h [29] whereas PLGA formulation gradually released the drug due to its hydrophobicity and as a consequence of its poor degradation in aqueous medium. It is inferred that the slow degradation of the polymer leads to continuous release of the drug [32]. Therefore, it is expected that the prepared nanosystem will be able to control drug delivery and protect drug molecules from biodegradability and plasma clearance.

At concentrations <100 μM, DMF drug has little lethal effect on splenocytes, and in higher concentrations, the survival rate decreases, which is similar to recent studies [35]. Statistical analysis shows that drug-free nanoparticles have no effect on cell viability as confirmed by previous investigations [36]. Drug-containing nanoparticles, and with significant difference, the antibody-bound nanoparticles containing drug have also shown little toxicity even at high concentrations and can therefore be considered as a non-toxic drug carrier. It's worth mentioning that, based on ISO standards, materials that do not induce the cytotoxicity greater than 30 % should be considered non-cytotoxic [37]. Lipopolysaccharide (LPS) LPS, a bacterial endotoxin, which upon binding to the surface of innate immune cells (e.g. dendritic cells) amplifies the secretion of pro-inflammatory cytokines (i.e., IL-1β, TNF-α, and IL-6) in a process called "cytokine storm" [38]. On the other hand, DMF exerts anti-inflammatory effects through suppressing LPS-induced mRNA expressions of TNF-α, IL-1β and IL-6 [39]. This phenotype was implemented to determine the efficacy of utilization of PLGA-NPs in delivering DMF. Real-time PCR test demonstrated that the expression at mRNA level of TNF-α, IL-1β and IL-6 decreased after treatment of splenocytes with DMF. The encapsulation of DMF into PLGA-NPs further enhanced DMF's anti-inflammatory effect, where it was more prominent in anti-CD40-mAb functionalized PLGA-NPs. DMF inhibits the activation of NFκB and ERK1/2 and thereby prevents the production of proinflammatory cytokines [40]. In similar studies, dimethyl fumarate inhibited the mRNA expression of NO, iNOS, IL-1β and TNF-α induced by LPS stimulation in microglia culture medium [25].

5. Conclusion

The present study was conducted to evaluate the effect of PLGA nanoparticles containing dimethyl fumarate on the expression of IL-1β, IL-6 and TNF-α cytokine genes in mouse splenocytes. Gene expression changed after treatment with various groups and differed from the untreated group. Drug-containing PLGA nanoparticles and PLGA nanoparticles containing drug bound to CD40 monoclonal antibody reduced expression in all cases as expected and were significant in some cases. There has always been ample evidence in previous studies indicating that DMF may have positive effects in reducing the expression of proinflammatory cytokines. We have shown that the delivery of sufficient amounts of this drug to target cells can play a greater role in regulating the expression of proinflammatory genes. CD40 s can be used as molecular targets for other therapeutic processes. Even the unique antioxidant and anti-inflammatory properties of DMF make it an interesting drug for testing other inflammatory conditions. On the other hand, since neurotransmitters released by neurons affect the activity of immune cells, the cytokines released by immune cells can in turn affect the function of nerve cells through cognate receptors on the surface of neurons. In addition, it has been widely accepted that the sympathetic nervous system (SNS) strongly innervates the spleen and that the synaptic nerve ends are in close contact with immune cells. The diffused neurotransmitters reach the surface of macrophages and/or lymphocytes, interacting with them through specific receptors and modulating the immune cell responses (e.g. inhibit or enhance the expression of various cytokines). This two-way neuroimmunity can be positive for therapeutic purposes.

Our results in this area are promising and provide a good basis for further future studies in this field.

CRediT authorship contribution statement

Sahar khosravi performed the experiments and analyzed the data; Hassan Bardania performed the experiments, analyzed the data and wrote the manuscript; Mohamad Hassan Fouani wrote the manuscript; Fereshteh Ghafari, Adel Mohammadzdeh, Ali Abbas Pourfathollah and Masoud Soleimani performed the experiments; Reza Mansouri, Mohammad Taher Tahoori designed the experiments, analyzed the data, and wrote the manuscript.

Declaration of Competing Interest

The authors declare that they have no conflict of interest.

Acknowledgments

This study was financially supported by a research grant from Iran National ScienceFoundation (INSF). This article is extracted from an MSc thesis approved at Shahid Sadoughi Medical School in Yazd. The authors take this opportunity to express their sincere gratitude to the research officials of Yazd Medical School and the dissertation jury who helped us to carry out and improve the quality of this research.

References

[1] A. Compston, A. Coles, Multiple sclerosis, Lancet 372 (2008) 1502–1517.
[2] A.M. Papini, E. König, Novel diagnostic tools and solutions for multiple sclerosis treatment: a patent review (2009-2014), Expert Opin. Ther. Pat. 25 (2015) 873–884.
[3] A.P. Robinson, C.T. Harp, A. Noronha, S.D. Miller, The experimental autoimmune encephalomyelitis (EAE) model of MS: utility for understanding disease pathophysiology and treatment, Handb. Clin. Neurol. 122 (2014) 173–189.
[4] R. Gold, R.A. Linker, M. Stangel, Fumaric acid and its esters: an emerging treatment for multiple sclerosis with antioxidative mechanism of action, Clin. Immunol. 142 (2012) 44–48.
[5] R. Bomprezzi, Dimethyl fumarate in the treatment of relapsing-remitting multiple sclerosis: an overview, Ther. Adv. Neurol. Disord. 8 (2015) 20–30.
[6] A. Bar-Or, R. Gold, L. Kappos, D.L. Arnold, G. Giovannoni, K. Selmaj, J. O'Gorman, M. Stephan, K.T. Dawson, Clinical efficacy of BG-12 (dimethyl fumarate) in patients with relapsing–remitting multiple sclerosis: subgroup analyses of the DEFINE study, J. Neurol. 260 (2013) 2297–2305.
[7] R.A. Linker, R. Gold, Dimethyl fumarate for treatment of multiple sclerosis: mechanism of action, effectiveness, and side effects, Curr. Neurol. Neurosci. Rep. 13 (2013) 394.
[8] A. Giusti, M. Giambuzzi, Management of dysphagia in patients affected by multiple sclerosis: state of the art, Neurol. Sci. 29 (Suppl. 4) (2008) S364–366.
[9] E. Esposito, R. Cortesi, M. Drechsler, J. Fan, B.M. Fu, L. Calderan, S. Mannucci, F. Boschi, C. Nastruzzi, Nanoformulations for dimethyl fumarate: physicochemical characterization and in vitro/in vivo behavior, Eur. J. Pharm. Biopharm. 115 (2017) 285–296.
[10] B. Sriramoju, R.K. Kanwar, J.R. Kanwar, Nanomedicine based nanoparticles for neurological disorders, Curr. Med. Chem. 21 (2014) 4154–4168.
[11] H. Gao, Z. Pang, X. Jiang, Targeted delivery of nano-therapeutics for major disorders of the central nervous system, Pharm. Res. 30 (2013) 2485–2498.
[12] J.C. Olivier, Drug transport to brain with targeted nanoparticles, NeuroRx 2 (2005) 108–119.
[13] M.N. Koopaei, R. Dinarvand, M. Amini, H. Rabbani, S. Emami, S.N. Ostad, F. Atyabi, Docetaxel immunonanocarriers as targeted delivery systems for HER 2-positive tumor cells: preparation, characterization, and cytotoxicity studies, Int. J. Nanomed. 6 (2011) 1903–1912.
[14] J.M. Barichello, M. Morishita, K. Takayama, T. Nagai, Encapsulation of hydrophilic and lipophilic drugs in PLGA nanoparticles by the nanoprecipitation method, Drug Dev. Ind. Pharm. 25 (1999) 471–476.
[15] M. Chountoulesi, C. Demetzos, Promising nanotechnology approaches in treatment of autoimmune diseases of central nervous system, Brain Sci. 10 (2020) 338.
[16] I. Tabansky, M.D. Messina, C. Bangeranye, J. Goldstein, K.M. Blitz-Shabbir, S. Machado, V. Jeganathan, P. Wright, S. Najjar, Y. Cao, Advancing drug delivery systems for the treatment of multiple sclerosis, Immunol. Res. 63 (2015) 58–69.
[17] Y. Li, J. Yuan, Q. Yang, W. Cao, X. Zhou, Y. Xie, H. Tu, Y. Zhang, S. Wang, Immunoliposome co-delivery of bufalin and anti-CD40 antibody adjuvant induces synergetic therapeutic efficacy against melanoma, Int. J. Nanomed. 9 (2014) 5683.
[18] L. Zhao, L. Liu, B. Guo, B. Zhu, Regulation of adaptive immune responses by guiding cell movements in the spleen, Front. Microbiol. 6 (2015) 645.
[19] D.K. Kaushik, A. Bhattacharya, R. Mirzaei, K.S. Rawji, Y. Ahn, J.M. Rho, V. W. Yong, Enhanced glycolytic metabolism supports transmigration of brain-infiltrating macrophages in multiple sclerosis, J. Clin. Invest. 129 (2019) 3277–3292.

[20] V. Bronte, M.J. Pittet, The spleen in local and systemic regulation of immunity, Immunity 39 (2013) 806–818.
[21] F. Cathomas, S.J. Russo, Brain-spleen connection aids antibody production, Nature 581 (2020) 142–143.
[22] A. Lori, M. Perrotta, G. Lembo, D. Carnevale, The spleen: a hub connecting nervous and immune systems in cardiovascular and metabolic diseases, Int. J. Mol. Sci. 18 (2017).
[23] P.A. McCarron, W.M. Marouf, D.J. Quinn, F. Fay, R.E. Burden, S.A. Olwill, C. J. Scott, Antibody targeting of camptothecin-loaded PLGA nanoparticles to tumor cells, Bioconjug. Chem. 19 (2008) 1561–1569.
[24] C.C. Moura, M.A. Segundo, J. Neves, S. Reis, B. Sarmento, Co-association of methotrexate and SPIONs into anti-CD64 antibody-conjugated PLGA nanoparticles for theranostic application, Int. J. Nanomed. 9 (2014) 4911–4922.
[25] H. Wilms, J. Sievers, U. Rickert, M. Rostami-Yazdi, U. Mrowietz, R. Lucius, Dimethylfumarate inhibits microglial and astrocytic inflammation by suppressing the synthesis of nitric oxide, IL-1beta, TNF-alpha and IL-6 in an in-vitro model of brain inflammation, J. Neuroinflammation 7 (2010) 30.
[26] S. Ojha, B. Kumar, Preparation and statistical modeling of solid lipid nanoparticles of dimethyl fumarate for better management of multiple sclerosis, Adv. Pharm. Bull. 8 (2018) 225–233.
[27] M. Garinot, V. Fiévez, V. Pourcelle, F. Stoffelbach, A. des Rieux, L. Plapied, I. Theate, H. Freichels, C. Jérôme, J. Marchand-Brynaert, Y.J. Schneider, V. Préat, PEGylated PLGA-based nanoparticles targeting M cells for oral vaccination, J. Control. Release 120 (2007) 195–204.
[28] S. Ojha, B. Kumar, Formulation and optimization of chitosan nanoparticles of dimethyl fumarate using box-behnken design, Int. J. Appl. Pharm. 8 (2016) 10–17.
[29] S. Ojha, B. Kumar, H. Chadha, Neuroprotective potential of dimethyl fumarate-loaded polymeric nanoparticles against multiple sclerosis, Indian J. Pharm. Sci. 81 (2019).
[30] M. Thondawada, A.D. Wadhwani, S.P. D, H.S. Rathore, R.C. Gupta, P. K. Chintamaneni, M.K. Samanta, A. Dubala, S. Varma, P.T. Krishnamurthy, K. Gowthamarajan, An effective treatment approach of DPP-IV inhibitor encapsulated polymeric nanoparticles conjugated with anti-CD-4 mAb for type 1 diabetes, Drug Dev. Ind. Pharm. 44 (2018) 1120–1129.
[31] P. Kocbek, N. Obermajer, M. Cegnar, J. Kos, J. Kristl, Targeting cancer cells using PLGA nanoparticles surface modified with monoclonal antibody, J. Control. Release 120 (2007) 18–26.
[32] S. Aggarwal, S. Gupta, D. Pabla, R.S.R. Murthy, Gemcitabine-loaded PLGA-PEG immunonanoparticles for targeted chemotherapy of pancreatic cancer, Cancer Nanotechnol. 4 (2013) 145–157.
[33] A. Platel, R. Carpentier, E. Becart, G. Mordacq, D. Betbeder, F. Nesslany, Influence of the surface charge of PLGA nanoparticles on their in vitro genotoxicity, cytotoxicity, ROS production and endocytosis, J. Appl. Toxicol. 36 (2016) 434–444.
[34] A. Schrade, V. Mailänder, S. Ritz, K. Landfester, U. Ziener, Surface roughness and charge influence the uptake of nanoparticles: fluorescently labeled pickering-type versus surfactant-stabilized nanoparticles, Macromol. Biosci. 12 (2012) 1459–1471.
[35] M. Campolo, G. Casili, M. Lanza, A. Filippone, I. Paterniti, S. Cuzzocrea, E. Esposito, Multiple mechanisms of dimethyl fumarate in amyloid β-induced neurotoxicity in human neuronal cells, J. Cell. Mol. Med. 22 (2018) 1081–1094.
[36] H. Gomari, M. Forouzandeh Moghadam, M. Soleimani, M. Ghavami, S. Khodashenas, Targeted delivery of doxorubicin to HER2 positive tumor models, Int. J. Nanomed. 14 (2019) 5679–5690.
[37] N. Zoghi, M.H. Fouani, H. Bagheri, M. Nikkhah, N. Asadi, Characterization of minocycline loaded chitosan/polyethylene glycol/glycerol blend films as antibacterial wound dressings, J. Appl. Polym. Sci. 138 (2021) 50781.
[38] E. Daguindau, T. Gautier, C. Chague, J.-P. Pais de Barros, V. Deckert, L. Lagrost, P. Saas, Is it time to reconsider the lipopolysaccharide paradigm in acute graft-versus-host disease? Front. Immunol. 8 (2017) 952.
[39] H.C. Paraiso, P.-C. Kuo, E.T. Curfman, H.J. Moon, R.D. Sweazey, J.-H. Yen, F.-L. Chang, I.-C. Yu, Dimethyl fumarate attenuates reactive microglia and long-term memory deficits following systemic immune challenge, J. Neuroinflammation 15 (2018) 1–14.
[40] V.A. McGuire, T. Ruiz-Zorrilla Diez, C.H. Emmerich, S. Strickson, M.S. Ritorto, R. V. Sutavani, A. Weiβ, K.F. Houslay, A. Knebel, P.J. Meakin, I.R. Phair, M.L. J. Ashford, M. Trost, J.S.C. Arthur, Dimethyl fumarate blocks pro-inflammatory cytokine production via inhibition of TLR induced M1 and K63 ubiquitin chain formation, Sci. Rep. 6 (2016) 31159.